Gallacher, K., Velha, P. , Paul, D.J. , MacLaren, I. , Myronov, M., and Leadley, D.R. (2012) *Ohmic contacts to n-type germanium with low specific contact resistivity.* Applied Physics Letters, 100 (2). 022113. ISSN 0003-6951

AIP | Applied Physics Letters

Ohmic contacts to n-type germanium with low specific contact resistivity

K. Gallacher, P. Velha, D. J. Paul, I. MacLaren, M. Myronov et al.

Citation: Appl. Phys. Lett. **100**, 022113 (2012); doi: 10.1063/1.3676667

View online: http://dx.doi.org/10.1063/1.3676667

View Table of Contents: http://apl.aip.org/resource/1/APPLAB/v100/i2

Published by the American Institute of Physics.

Ohmic contacts to n-type germanium with low specific contact resistivity

K. Gallacher,[1] P. Velha,[1] D. J. Paul,[1,a)] I. MacLaren,[2] M. Myronov,[3] and D. R. Leadley[3]
[1]University of Glasgow, School of Engineering, Rankine Building, Oakfield Avenue, Glasgow G12 8LT, United Kingdom
[2]University of Glasgow, School of Physics and Astronomy, Kelvin Building, University Avenue, Glasgow G12 8QQ, United Kingdom
[3]University of Warwick, Department of Physics, Coventry CV4 7AL, United Kingdom

(Received 6 December 2011; accepted 22 December 2011; published online 13 January 2012)

A low temperature nickel process has been developed that produces Ohmic contacts to n-type germanium with specific contact resistivities down to $(2.3 \pm 1.8) \times 10^{-7}$ Ω-cm^2 for anneal temperatures of 340 °C. The low contact resistivity is attributed to the low resistivity NiGe phase which was identified using electron diffraction in a transmission electron microscope. Electrical results indicate that the linear Ohmic behaviour of the contact is attributed to quantum mechanical tunnelling through the Schottky barrier formed between the NiGe alloy and the heavily doped n-Ge. © *2012 American Institute of Physics*. [doi:10.1063/1.3676667]

There is presently increased interest in using Ge for both electronic and optical devices on top of Si substrates to expand the functionality of Si technology. Ge CMOS is being investigated for end-of-roadmap electronic devices where the high mobility of Ge potentially allows reduced-power operation,[1] epitaxial Ge on Si is being used as a photodetector for 1.55 μm telecoms,[2] and Ni contacts on Ge are being investigated for spintronic devices.[3] For all these applications, low resistivity n- and p-type Ohmic contacts are essential for high performance devices and circuits. For the integration of Ge into such applications, the challenges faced are poor solubility of dopants, large diffusion coefficients, and the incomplete activation of dopants which have led to high off currents and low on-drive currents in transistors.[4] The poor device performances have all stemmed from the large contact resistances found in the source and drain regions. The large contact resistances to n-Ge have been attributed to Fermi level (E_F) pinning near the valence band which results in large Schottky barrier heights (SBH) independent of the metal work function.[5]

Most of the previous work on n-Ge contacts has focussed on reducing the SBH by alleviating the E_F pinning either by insertion of an interfacial layer or by passivating the n-Ge surface. Whilst the cause of E_F pinning is still not fully understood, the metal induced gap states (MIGS)[5] theory explains the consequences. The free electron wave function from the metal penetrates into the semiconductor bandgap inducing gap states that are either acceptor or donor like states. Depending on the surface state distribution and the E_F of the semiconductor, these states will be partially filled and can lead to a positive or negative net surface charge. The position of the E_F at which the surface is electrically neutral is called the charge neutrality level (CNL). For Ge, the CNL occurs just above the valence band, where the metal E_F is pinned in energy, and so, large SBHs are predicted for metals deposited onto n-type Ge (see Fig. 1(a)). Using the MIGS theory, a number of methods have been used to suppress the metal wave function from penetrating into the Ge to reduce the specific contact resistivity, ρ_c. They are based on the concept of inserting an interfacial layer such as Al_2O_3,[6] Ge_3N_4,[7] Si_3N_4,[8] or Si (Ref. 9) between the metal and the n-Ge and have shown promise in reducing the SBH, but the ρ_c have remained relatively high ($\rho_c \geq 2 \times 10^{-6}$ Ω-cm^2)[9] due to the resistance of the inserted interfacial layer. Dimoulas and Nishimura investigated a wide range of metal/n-Ge contacts and found that the SBH is relatively independent of its work function and ranges from 0.5-0.6 eV.[10,11] The ideal way to overcome large SBH normally focuses on having extremely high doping as the Schottky barrier width is inversely proportional to doping, therefore, a narrow Schottky barrier width allows tunnelling of electrons through the barrier (Fig. 1(b)) and metal contacts with good electrical behaviour.

In this work, Ohmic contacts with ρ_c down to $(2.3 \pm 1.8) \times 10^{-7}$ Ω-cm^2 were demonstrated using the direct deposition of Ni onto n-type Ge with a measured doping density of 3×10^{19} cm^3 followed by a low temperature anneal. The n-Ge material was epitaxially grown using an ASM Epsilon 2000E low pressure chemical vapour deposition tool. A 650 nm strain relaxed virtual substrate of undoped Ge was directly grown onto a 200 mm p$^-$-Si (001) wafer using the two-temperature method[12] followed by a 830 °C anneal to reduce the threading dislocation density to around 10^7 cm^{-2}. Then, 300 nm of n-type phosphorus-doped Ge with $N_D \approx 3 \times 10^{19}$ cm^{-3} was grown. 1 cm^2 samples for electrical measurements were prepared by first cleaning in acetone followed by a rinse in propan-2-ol, and then, the native oxide was removed in a buffered hydrofluoric acid (BHF) solution (5:1). The samples were then immediately placed in a high vacuum (5×10^{-7} Torr) metal deposition system before 100 nm of Ni was deposited by electron-beam evaporation and patterned by a lift-off process. Samples were produced using electron beam lithography in a Vistec VB6 tool to produce devices with placement accuracy of ~1 nm. Ni was chosen as it reacts at a relatively low temperature (<400 °C), is stable over a wide temperature range, has the lowest sheet resistance, R_{sh}, of most of the common transition metal-germanium alloys, does not easily oxidise, and has electrical

a)Electronic mail: Douglas.Paul@glasgow.ac.uk.

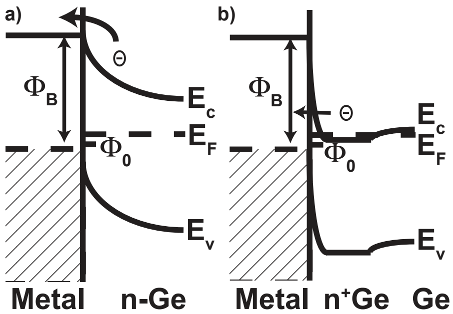

FIG. 1. (a) The normal case for a metal contact to lightly doped n-Ge where the E_F is pinned near the CNL (Φ_0) which is located just above the valence band and therefore induces a large SBH (Φ_B) regardless of the metal work function. (b) In our case, the material is doped sufficiently to reduce the barrier width to allow tunnelling of electrons.

resistivity phases that have comparable electrical values to nickel silicides.[13] 100 nm thin films were used as it allowed the contacts to be characterized over a wide range of anneal temperatures. All annealing was performed in a rapid thermal annealer (RTA) using N_2 and anneal temperatures ranged from 300-600 °C for 30 s. Electrical measurements using 4 point probe techniques, transmission line measurements (TLMs), and Hall effect measurements on mesa etched Hall bar samples all produced nominally identical resistivities of 0.7×10^{-3} Ω-cm indicating a doping density of 3×10^{19} cm^{-3} if it is assumed that all the dopants are activated. Due to the large dopant concentration (see Fig. 1(b)), thermionic emission will not be the only conduction mechanism. Since the Schottky barrier width is inversely proportional to the doping density in the Ge, this width is expected to be small enough to allow quantum mechanical tunnelling for doping densities above 10^{19} cm^{-3} (see Fig. 1(b)).

Electrical characterization of the Ni-Ge contacts was carried out using the circular transfer length method (CTLM).[14] The CTLM is a self isolating structure, and therefore, no mesa etch is required to prevent current crowding which affects other planar test structures such as the cross-bridge Kelvin resistor and the standard linear TLM. CTLM structures allow extraction from extrapolation of the contact resistance, transfer length, and sheet resistance from which the ρ_c can be calculated. The structure consists of a metallic outer region and an inner circular contact of radius L. A gap spacing of d separates the inner and outer regions. By measuring the total resistance for each gap spacing and using a correction factor C to compensate for the difference between the linear transfer method and the CTLM to obtain a linear fit to the experimental data, without the correction factor, CTLMs underestimate the ρ_c. From this, the sheet resistance, contact resistance, and the transfer length can be calculated. CTLMs had inner contact radius ranging from 75-125 μm, and gap spacing varied from 10-200 μm. Measured current-voltage characteristics are shown in Fig. 2(a). As can be observed from Fig. 2, the Ni-Ge contact annealed at 340 °C is clearly Ohmic at room temperature and also at 77 K. The current-voltage characteristics show that the tunnelling current is the dominant transport mechanism. Fig. 2(b) shows a measurement of a 100 μm CTLM for a Ni-Ge contact annealed at 340 °C. The plot shows total resistance, R_T, versus gap spacing for corrected and uncorrected data where

$$R_T = \frac{R_{sh}}{2\pi}[d + 2L_T]C \text{ with } C = \frac{L}{d}\ln\left(1 + \frac{d}{L}\right), \quad (1)$$

L_T is the transfer length, and $\rho_c = L_T^2 R_{sh}$.[12]

Fig. 3 shows how ρ_c varies as a function of anneal temperature. The lowest values of $\rho_c = 2.3 \pm 1.8 \times 10^{-7}$ Ω-cm^2 occur at 340 °C with $L_T = 1.2 \pm 0.45$ μm and $R_{sh} = 19.0 \pm 0.2$ Ω and are lower than previously published results[5–9] whilst using a simpler process. The phase diagram for Ni-Ge alloys is quite complicated[15] with multiple phases that can grow

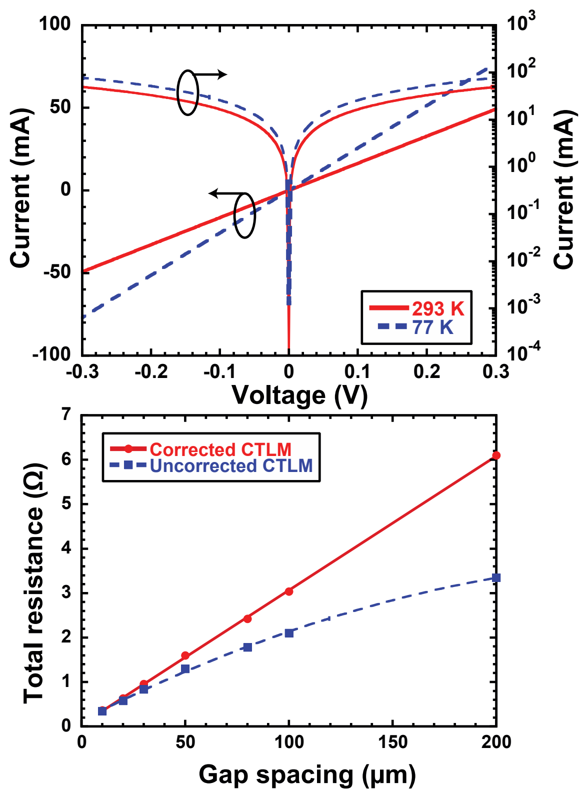

FIG. 2. (Color online) (a) The left axis shows the linear current-voltage of the CTLM (L = 100 μm, d = 150 μm) at 293 K (solid line) and at 77 K (dashed line) for a NiGe/Ge(100) contact annealed at 340 °C for 30 s, and the right axis is a log plot. (b) The total 2 terminal resistance as a function of gap spacing for CTLMs.

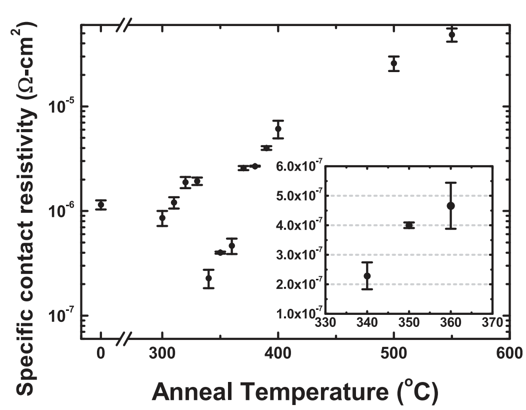

FIG. 3. Calculated ρ_c for a 100 nm Ni film on n-Ge contacts over the anneal temperature range 0-600 °C. The inset shows in more detail the results with the lowest values.

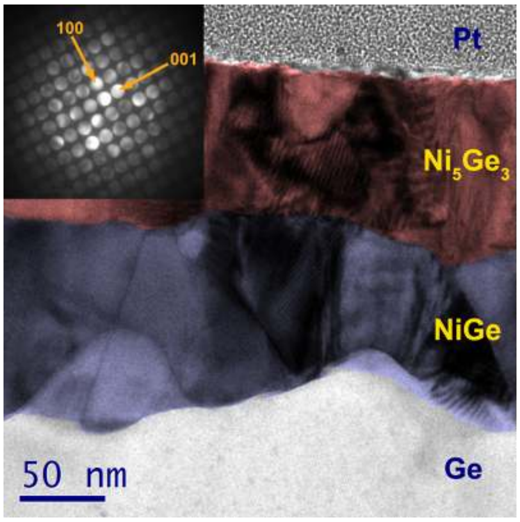

FIG. 4. (Color online) A TEM bright field image of a Ni-Ge contact annealed at 340 °C showing the 2 layers of the contact on the Ge substrate. False colour shading was used to highlight the 2 layers of the alloy contact. The amorphous Pt on top protects the sample prior to preparation by a focused ion beam lift-out process. The insert is a convergent beam diffraction pattern from 1 grain of the lower layer consistent with the [010] zone axis of NiGe in the orthorhombic (Pnma) structure.[16]

simultaneously, in particular Ni_5Ge_3 and NiGe.[13,17,18] The first phase is a Ni rich phase of Ni_5Ge_3 followed by a stoichiometric NiGe phase. Results have shown that NiGe is present after the electron-beam evaporation of Ni onto amorphous and polycrystalline Ge without annealing,[17] and the unannealed results in Fig. 3 suggest NiGe may have formed during the evaporation in the present work. Therefore, NiGe if formed during deposition and isothermal annealing leads to the simultaneous growth of Ni_5Ge_3 and NiGe in the presence of Ni after a critical thickness of 10-20 nm is reached for Ni_5Ge_3.[17,18]

To fully understand which phase is producing the lowest ρ_c values, transmission electron microscopy (TEM) was undertaken on a sample annealed at 340 °C using a FEI Tecnai T20 operated at 200 kV for imaging and diffraction and a FEI Tecnai TF20 operated at 200 kV with an energy dispersive analysis x-ray (EDAX) spectrometer for energy dispersive x-ray spectrometry (EDXS). Fig. 4 shows a typical bright field image showing that the contact consists of two distinct layers. The lower layer in direct contact to the n-Ge was shown by EDXS and diffraction (inset) to be the lower resistivity NiGe phase with an average composition from five quantified spectra of 50 ± 2% Ni and 50 ± 2% Ge. The upper layer was shown by EDXS to be the higher resistivity Ni_5Ge_3 phase, with the average of 5 spectra giving 63 ± 3% Ni and 37 ± 3% Ge in excellent agreement with expectations for Ni_5Ge_3. The diffraction patterns are also consistent with this phase.[13]

To conclude, Ohmic contacts with ρ_c down to $(2.3 \pm 1.8) \times 10^{-7}$ Ω-cm^2 have been demonstrated on n-Ge using a Ni metal process annealed at 340 °C. Electron diffraction in a TEM indicates the formation of the low resistivity NiGe phase. Further work is required to improve the performance of the contacts formed by this process. In particular, methods are required which produce only the low resistivity NiGe phase as well as a smooth NiGe/n-Ge interface at the nanoscale level.

This work was supported by the UK EPSRC.

[1]R. Pillarisetty, Nature **479**, 324 (2011).
[2]D. J. Paul, Electron. Lett. **45**, 582 (2009).
[3]C. Shen, T. Trypiniotis, K. Y. Lee, S. N. Holmes, R. Mansell, M. Husain, V. Shah, X. V. Li, H. Kurebayashi, I. Farrer, C. H. de Groot, D. R. Leadley, G. Bell, E. H. C. Parker, T. Whall, D. A. Ritchie, and C. H. W. Barnes, Appl. Phys. Lett. **97**, 162104 (2010).
[4]H. Shang, L. Kam-Leung, P. Kozlowski, C. D'Emic, I. Babich, E. Sikorski, L. Meikei, H.-S. P. Wong, K. Guarini, and W. Haensch, IEEE Electron Device Lett. **25**, 135 (2004).
[5]J. F. Wager and J. Robertson, J. Appl. Phys. **109**, 094501 (2011).
[6]L. Lin, J. Robertson, and S. J. Clark, Microelectron. Eng. **88**, 1461 (2011).
[7]R. R. S. Lieten, S. Degroote, M. Kuijk, and G. Borghs, Appl. Phys. Lett. **92**, 022106 (2008).
[8]M. Kobayashi, A. Kinoshita, K. Saraswat, H.-S. P. Wong, and Y. Nishi, J. Appl. Phys. **105**, 023702 (2009).
[9]K. Martens, R. Rooyackers, A. Firrincieli, B. Vincent, R. Loo, B. De Jaeger, M. Meuris, P. Favia, H. Bender, B. Douhard, W. Vandervorst, E. Simoen, M. Jurczak, D. J. Wouters, and J. A. Kittl, Appl. Phys. Lett. **98**, 013504 (2011).
[10]A. Dimoulas, P. Tsipas, A. Sotiropoulos, and E. K. Evangelou, Appl. Phys. Lett. **89**, 252110 (2006).
[11]T. Nishimura, K. Kita, and A. Toriumi, Appl. Phys. Lett. **91**, 123123 (2007).
[12]V. A. Shah, A. Dobbie, M. Myronov, and D. R. Leadley, Solid-State Electron. **62**, 189 (2011).
[13]S. Gaudet, C. Detavernier, A. J. Kellock, P. Desjardins, and C. Lavoie, J. Vac. Sci. Technol. A **24**, 474 (2006).
[14]D. K. Schroder, *Semiconductor Material and Device Characterisation*, 3rd ed. (John Wiley & Sons, Hoboken, New Jersey, 2006).
[15]T. B. Massalski, *Binary Alloy Phase Diagram* (ASM, Materials Park, OH, 1986).
[16]H. Pfisterer and K. Schubert, Zeitschrift für Metallkunde **41**, 358 (1950).
[17]F. Nemouchi, D. Mangelinck, C. Bergman, G. Clugnet, P. Gas, and J. L. Lábár, Appl. Phys. Lett. **89**, 131920 (2006).
[18]F. Nemouchi, D. Mangelinck, J. L. Lábár, M. Putero, C. Bergman, and P. Gas, Microelectron. Eng. **83**, 2101 (2006).